Ionic basis of a differential effect of adenosine on refractoriness in rabbit AV nodal and atrial isolated myocytes

Antony J. Workman, Kathy A. Kane *, Andrew C. Rankin

Department of Medical Cardiology, Royal Infirmary, 10 Alexandra Parade, Glasgow G31 2ER, UK

** Department of Physiology and Pharmacology, University of Strathclyde, Strathclyde Institute for Biomedical Sciences, 27 Taylor Street, Glasgow G4 ONR , UK*

Address for correspondence and proofs:

Dr Antony John Workman

Department of Medical Cardiology

Royal Infirmary

10 Alexandra Parade

Glasgow G31 2ER

UK

Tel: +44 (0) 141 211 1231

Fax: +44 (0) 141 552 4683

Abstract

Antony J. Workman, Kathy A. Kane, Andrew C. Rankin. Ionic basis of a differential effect of adenosine on refractoriness in rabbit AV nodal and atrial isolated myocytes

Objectives: Firstly, to compare effects of adenosine on membrane potential and refractoriness in AV nodal and atrial cells. Secondly, to assess the contribution of the effects of adenosine on I_{KAdo} and I_{CaL} to its effects on the functional electrophysiological properties in the two cell types. **Methods:** The whole cell patch clamp technique was used to record action potentials and ion currents in AV nodal and left atrial myocytes isolated enzymatically from rabbit hearts. **Results:** Adenosine (10 μM) caused similar hyperpolarisation and shortening of the action potential duration (APD) in both cell types: maximum diastolic potential was hyperpolarised from -59±3 to -66±2 and from -70±2 to -76±2 mV (mean±SEM) and APD_{90} was shortened by 31±4 and 30±7 % in AV nodal (*n*=14) and atrial cells (*n*=8), respectively. Adenosine shortened the effective refractory period (ERP) in atrial cells, from 124±15 to 98±14 ms (*n*=8). In contrast, ERP in AV nodal cells was not significantly affected (112±13 vs 102±12 ms, *n*=14), and post-repolarisation refractoriness was prolonged. By contrast, current injection, to induce an equal degree of hyperpolarisation to that produced by adenosine, shortened APD and ERP in both cell types, suggesting an additional action of adenosine in AV nodal cells. Adenosine (10 μM) did not affect peak I_{CaL} in AV nodal cells, but significantly altered the biexponential time course of recovery of I_{CaL} from inactivation. The proportion of recovery in the fast phase (time constant, τ=102±10 ms) was reduced from 71±3 to 55±5 %, with shift to the slow phase (τ=858±168 ms), without altering τ in either phase. A similar effect of adenosine was seen in left atrial cells. **Conclusion:** Adenosine caused hyperpolarisation, APD-shortening and slowing of recovery of I_{CaL} from inactivation, in both AV nodal and atrial cells, but prolonged post-repolarisation refractoriness in AV nodal cells only. This differential effect of adenosine on refractoriness in the two cell types could not be explained by effects on I_{KAdo}, but may be due to slowed reactivation of I_{CaL}, which is the predominant inward current in AV nodal but not left atrial cells.

Keywords

Discipline of study: Experimental

Object of study: Heart

Level of study: Cellular

Field of study: Electrophysiology

5 additional keywords: Adenosine; AV-node; Rabbit; Myocytes; Membrane currents

1. Introduction

Adenosine exerts complex electrophysiological effects on the myocardium, which are cell-type specific. In most mammalian species, exogenous adenosine has no effect on ventricular action potentials, but exerts various effects on action potentials recorded from supraventricular myocardium [1]. In the atrioventricular (AV) node, adenosine has a negative dromotropic effect, evident electrophysiologically as conduction slowing (prolongation of the atrio-His interval), or complete AV block with sufficiently high concentrations of extracellular adenosine [2]. This forms the basis of the clinical anti-arrhythmic actions of adenosine. For example, when injected as an intravenous bolus, adenosine converts the majority of paroxysmal supraventricular tachycardias, which involve the AV node in a reentrant circuit, to normal sinus rhythm [3].

Adenosine-induced AV nodal conduction block may be mediated by a complex interaction of effects on AV nodal excitability and refractoriness. In the intact node of the rabbit and guinea-pig, adenosine has been demonstrated to prolong the AV nodal effective refractory period ERP [4]. The cellular basis of these functional effects of adenosine has not been extensively studied. A single study [5], has shown that adenosine depressed excitability and produced a small prolongation of ERP in single AV nodal cells. In the atrium, in contrast to the AV node, adenosine shortens the ERP, in conjunction with shortening of the action potential duration (APD) [5,6]. The first aim of the present study was to compare the effects of adenosine on membrane potential and refractoriness in AV nodal and atrial cells.

With respect to the ionic basis of these functional effects, adenosine activates an inwardly rectifying K^+ current (I_{KAdo}) in atrial [7] and AV nodal cells [8]. This current, shown at the single channel level to be the same as that activated by acetylcholine [9], has been demonstrated to cause hyperpolarisation and shortening of the APD in AV nodal cells [8] and in atrial myocytes [10]. In addition, adenosine exerts effects on the Ca^{2+} current (I_{Ca}). In particular, it has a marked anti-adrenergic effect on the L-type Ca^{2+} current, I_{CaL} [11]. The effect of adenosine on basal (non β-adrenergically stimulated) I_{CaL} in AV nodal cells is variable [8], or required high concentrations of adenosine [5]. Thus, the second aim of the study was to assess the

contribution of the effects of adenosine on I_{KAdo} and I_{CaL} to its effects on the functional properties of membrane potential and refractoriness in AV nodal and atrial cells.

2. Methods

2.1. Isolation of single AV nodal and atrial myocytes

Cells were isolated from both the AV nodal region and the left atrium of rabbit hearts, using a method modified from that previously described [8]. The investigation conforms with the *Guide for the Care and Use of Laboratory Animals* published by the US National Institutes of Health (NIH Publication No. 85-23, revised 1996). New Zealand white male rabbits (2-3.5 kg) were administered a lethal dose of anaesthetic (100 mg/kg sodium pentobarbitone, intravenous injection), and heparinised with 335 U/kg heparin. The heart was excised and retrogradely perfused via the aorta for 10 min, with a physiological salt solution (see *Solutions*, below) at a constant flow rate of 25 ml/min, at 37^{o}C. The heart was then perfused for a further 4 min, with 0.73 mg/ml collagenase (Type 1; 296 U/mg, Worthington), 0.1 mg/ml protease (Type XIV; 4.6 u/mg, Sigma) and $CaCl_2$ (67 μM) added, with the coronary effluent being recirculated after 1 min. The heart was pinned out on a dissecting dish and the right atrium opened. The partially digested AV nodal region, demarcated by the tricuspid valve inferiorly, the tendon of Todaro superiorly, the coronary sinus posteriorly and central fibrous body anteriorly, was removed. The left atrial appendage was removed at this stage and treated identically to, but separate from, the AV nodal region. The tissue to be digested was chopped into 1 mm^3 pieces and placed into a flask containing 1.5 ml of recirculated enzyme solution with 1.5 % bovine albumin (Fraction V, Sigma). Cells were then mechanically disaggregated using a shaking water bath (Grant OLS 200), with orbital shaking (130 revolutions/min) at 37 ^{o}C. After 5 min, and then a further 5 min, the cell suspension was filtered through nylon gauze (200 μm mesh, Barr & Wray, Lanark, UK) and centrifuged at 80 g for 2 min. Cells were resuspended in 3 ml of the physiological salt solution containing 0.5 mM $CaCl_2$ plus 1.5 % albumin, and allowed to sediment for 15 min. The supernatant was replaced and the $CaCl_2$ concentration was sequentially increased, to 1 mM after 15 min, then to 2 mM after a further 30 min. Finally, cells were stored at room temperature for up to 18 hr in a culture medium containing 2 mM $CaCl_2$ (M199, Gibco BRL).

2.2. Solutions

All solutions were made with "ultrapure" water, treated by reverse osmosis (Milli-Ro Plus and Milli-Q, Millipore) and using Analar grade chemicals. The solution for isolating cells contained (mM): NaCl (130), KCl (5.4), $MgCl_2.6H_2O$ (3.5), $NaH_2PO_4.H_2O$ (0.45), HEPES (5), glucose (11.1), taurine (20) and creatine hydrate (10), bubbled with 100 % O_2, pH 7.25. The cell superfusion solution contained (mM): NaCl (130), KCl (4), $CaCl_2$ (2), $MgCl_2$ (1), glucose (10), HEPES (10), pH 7.36. Electrode filling solutions were either aspartate-based, containing (mM): L-aspartic acid (110), KCl (20), $MgCl_2$ (1), EGTA (0.15), Na_2ATP (4), Na_2GTP (0.4), HEPES (5), pH 7.25, or Cs^+-based, with the KCl and L-aspartic acid substituted with CsCl (130 mM).

2.3. Electrical recording techniques

Aliquots of cell suspension were transferred by Pasteur pipette to a fast exchange (<10 s) perfusion chamber of 200 μl volume (RC-24E, Warner), mounted on the stage of an inverted microscope (TMS, Nikon). Cells were allowed to sediment for 10-15 min, before superfusing at 35-37 ^oC at approx. 1.5 ml/min, via an in-line solution heater (SH-27G, Warner) with gravity feed. Action potentials and ion currents were recorded using the whole cell patch clamp technique, with an Axopatch-1D amplifier (Axon Instruments). Microelectrodes were pulled by gravity from thin walled, filamented borosilicate glass tubes (Clark Electromedical) to resistances of 4-8 MΩ, using a vertical micropipette puller (Narishige PP-83) and fire-polished. Action potentials were stimulated and recorded by current clamping, using the aspartate-based pipette solution. With this solution, a liquid junction potential of +7±0.3 mV (bath relative to pipette, *n*=6) was measured, and compensated for prior to seal formation [12]. Stimulating pulses were 1.2x threshold strength, and of 5 ms duration. Ca^{2+} currents were recorded by voltage clamping, using the Nystatin perforated patch technique [13], because of previously observed rundown of I_{CaL} using ruptured patches [8]. Nystatin (184 μM, Sigma) was prepared hourly, and the Cs^+-based pipette solution was used to abolish outward K^+ currents. With this solution, no significant liquid junction potential occurred (+0.2±0.2 mV, *n*=5) and so no compensation was

necessary. Following seal formation, a gradual reduction in the series resistance due to Nystatin pore formation was continuously monitored, until stabilisation occurred (after approximately 7 min) at 3-8 MΩ. The series resistance was routinely electronically compensated for (by 67-84 %). The L-type Ca^{2+} current was activated with voltage pulses to +10 mV, from a holding potential of -40 mV. Cells were both stimulated, and recorded from, using "WinWCP", a software program written by John Dempster, Strathclyde University. Current and voltage signals were filtered at 5 kHz, monitored on an oscilloscope (Farnell DTS 20), and digitised (National Instruments LAB-PC A-D converter), for storage on a computer.

2.4. Experimental protocols

The cell input resistance was initially measured in each cell, by voltage clamping with a voltage ramp (from -120 mV to +50 mV in 7 s), from the slope of the linear part of the resulting whole cell current, usually between -90 and -120 mV. The AV nodal sample inevitably contained right atrial cells also, which may show similar morphology and electrophysiology to atrio-nodal (A-N) AV nodal cells [14]. Therefore, since AV nodal cells have a high input resistance (due to lack of inward rectifier current, I_{K1}), a high input resistance was used to distinguish AV nodal cells from other cell types. In a previous study on rabbit AV nodal cells the input resistance, also measured from the linear part of the current-voltage relationship, i.e.: at potentials substantially more negative than the zero current potential, was approximately 230 MΩ [5]. Based on this, and on studies in which cells were identified as AV nodal also on the basis of their input resistances [15,16], we accepted cells as AV nodal if their input resistance was >180 MΩ. In contrast to some of the AV nodal cells, all atrial cells were quiescent, and the maximum diastolic and resting potentials, respectively, of these cell types, is referred to throughout as the maximum diastolic potential (MDP).

The ERP was determined using a train of 8 conditioning current pulses (S_1), delivered at a rate of 300 beats/min, preceding a premature pulse (S_2) of the same magnitude. The S_1-S_2 interval was shortened by 10 ms intervals and the ERP was defined as the longest S_1-S_2 interval which failed to elicit an S_2 action potential of amplitude >80 % of the preceding S_1 action potential. The stimulus current magnitude required

to cause a regenerative action potential response (the threshold current) was determined using a stimulation protocol similar to that for measuring ERP, except that the S_1-S_2 current pulse interval was kept constant at 200 ms (the same as the S_1-S_1 interval), and the magnitude of the S_2 pulse was progressively increased from zero, in steps of 50 pA, until an action potential occurred. The maximum rate of rise of the action potential upstroke (dV/dt)max is referred to throughout as V_{max}. This was measured after any initial upstroke artifact caused by the current pulse. In a few cells, V_{max} measurement was not attempted due to possible interference from a current pulse artifact. The Axopatch-1D is a current follower, providing accurate measurement of V_{max} of ≤60 V/s. V_{max} measurements >60 V/s, however, may have been underestimated by the use of this amplifier.

The effect of hyperpolarisation on action potentials, ERP and threshold current was determined by injecting a hyperpolarising current, in current clamp mode. The magnitude of this current was measured in each cell prior to performing the current clamp protocols, by iteratively adjusting the holding current, until the required degree of hyperpolarisation was attained. Cells were then allowed to recover for 1 min. Current injection was started 30 s before recordings were made, and recovery was assessed 30 s after current injection was ceased.

The magnitude of peak I_{CaL} and the time course of recovery of I_{CaL} from inactivation were determined using a double voltage pulse protocol. An initial 1 s conditioning voltage pulse to +10 mV was followed by a 300 ms test pulse. The interpulse interval, *t* was progressively reduced from 3 s to 20 ms, in steps of 20 or 50 ms (see inset of Fig. 4B). There was a 6 s delay between applying each pulse pair. Current kinetics data were analysed using curve-fitting, with the following equation:

$$Y=Ymax_1[1-\exp(-x/\tau_1)]+Ymax_2[1-\exp(-x/\tau_2)],$$

where $Y=I_{CaL}$ amplitude (% of maximum value, recorded at interpulse interval of 3 s); $Ymax_1$ and $Ymax_2$=plateaux of I_{CaL} amplitude in the 1st and 2nd phases of recovery, respectively (% of maximum value,

recorded at interpulse interval of 3 s); x=time (ms), and τ_1 and τ_2=time constants (ms) for 1st and 2nd phases of recovery, respectively.

Protocols were repeated (except for hyperpolarising current injection) after superfusing cells for 90 s with adenosine (10 μM), and again 180 s after removal of adenosine from the recording chamber. This concentration of adenosine was chosen because previous work [8] has shown that 10 μM is a sub-maximally effective concentration in rabbit AV nodal cells.

2.5. Data analysis and statistics

Voltage and current traces were analysed "off-line" using the software program "WinWCP", written by John Dempster, Strathclyde University, UK. Electrophysiological changes due to interventions were included in the analysis only if these could be shown to be reversible on removal of the intervention. Values were expressed as mean±SEM. Differences between values were assessed using two-tailed paired or unpaired Student's *t* tests, as appropriate. Differences in goodness of fit were assessed when using non-linear regression, using an F test. $P<0.05$ was regarded as statistically significant.

3. Results

3.1. Electrophysiological characteristics of AV nodal and left atrial myocytes

Differences in the electrophysiology of AV nodal and left atrial myocytes are illustrated in the left hand panels of Fig. 1A. The last action potential of the conditioning trains from an AV nodal (Fig. 1Ai) and an atrial myocyte (Fig. 1Aii), followed by the first action potentials evoked by the test pulses, are shown. The longest coupling interval which failed to elicit a response is shown in each case, and reflects the ERP. It can be seen that the AV nodal action potential had a slower upstroke velocity and a lower amplitude compared to that of the atrial myocyte. The maximal rate of rise was 50±10 versus 162±16 V/s (P<0.05) and the amplitude was 84±4 versus 121±5 mV (P<0.05) for the AV nodal cells (n=35) and left atrial cells (n=20), respectively. The AV nodal cells had a more positive maximum diastolic potential (-57±2 mV, n=35) than the left atrial cells (-70±1 mV, n=20, P<0.05), and a higher input resistance (421±39 vs 105±15 MΩ, P<0.05). In none of the atrial cells was the input resistance >180 MΩ. The action potential duration at both 50 and 90 % repolarisation (APD_{50} and APD_{90}, respectively), was similar in AV nodal cells and left atrial cells (left hand panels of Fig. 1A). Mean APD_{50} was 43±3 and 45±6 ms in AV nodal and left atrial cells, respectively, while mean APD_{90} was 82±4 and 91±7 ms, in AV nodal and atrial cells (n=35 and 20), respectively. Non-electrophysiological characteristics also differed between the two cell types. The AV nodal cells, the majority of which appeared "spindle-shaped", were thinner and usually shorter than the atrial cells. AV nodal cell mean maximum width (9±1 μm, n=24) and length (97±4 μm, n=24) were significantly (P<0.05) lower than the corresponding values in atrial cells (14±1 and 120±4 μm, n=30). This was associated with a significantly smaller capacity in AV nodal cells (56±2 pF, n=39) than atrial cells (83±3 pF, n=34; P<0.05).

AV nodal cells, in contrast to left atrial cells, displayed marked post-repolarisation refractoriness, as shown in Fig. 1A. In the AV nodal cell (Fig. 1Ai) the first action potentials to fire in response to the premature stimuli (S_2) occur well after full repolarisation of the preceding action potentials. In the left atrial cell,

however (Fig. 1Aii), the first action potentials fire earlier after the last action potential of the conditioning train, before full repolarisation. The mean values of the ERP were similar (140±7 ms, *n*=35 in AV nodal cells, and 125±7 ms, *n*=20 in the left atrial cells). However, the mean ratio of ERP/APD_{90}, an index of post-repolarisation refractoriness, was significantly greater in AV nodal, than in left atrial cells (1.71±0.06 vs 1.45±0.07, $P<0.05$).

The V_{max} value of individual AV nodal cells was variable (*n*=35). In 15 of these cells, V_{max} was <15 V/s, suggestive of nodal (N), or nodal-His (N-H) cells. Therefore, the population of AV nodal cells was subdivided into "slow V_{max}" cells (V_{max} <15 V/s, *n*=15), eg: Fig. 1Ai (V_{max} = 4.5 V/s), and "fast V_{max}" cells, which may correspond to A-N cells (V_{max} >15 V/s, *n*=20), to see if these two cell populations displayed different responses in subsequent experiments. The mean V_{max} values of the slow and fast V_{max} AV nodal cells were 7.3±0.9 and 82±13 V/s, respectively. The slow V_{max} cells had a more positive maximum diastolic potential than the fast V_{max} cells, at -51±2 vs -62±2 mV ($P<0.05$) and also had a smaller amplitude (71±4 vs 94±5 mV; $P<0.05$). The APD_{50} and APD_{90} of the slow V_{max} cells, at 49±3 and 88±3 ms, respectively, were not significantly different from those of the fast V_{max} cells (39±5 and 78±6 ms, respectively). However, both the ERP and the ERP/APD_{90} ratio of the slow V_{max} cells, at 166±6 ms, and 1.91±0.09, respectively, were significantly greater that those of the fast V_{max} cells (120±10 ms and 1.57±0.06, respectively; $P<0.05$). This indicated pronounced post-repolarisation refractoriness in the slow V_{max} cells. The fast V_{max} AV nodal cells were clearly distinct from the left atrial cells, with a slower V_{max} (82±13 vs 162±15 V/s; $P<0.05$) and a higher input resistance (366±39 vs 103±28 MΩ; $P<0.05$).

3.2. Effects of adenosine on action potentials and ERP

Adenosine (10 μM) hyperpolarised the maximum diastolic potential and shortened APD, in both AV nodal and left atrial cells (right hand panels of Fig. 1A). The mean maximum diastolic potential was significantly hyperpolarised from -59±3 to -66±2 mV in AV nodal cells ($P<0.05$, *n*=14), and from -70±2 to -76±2 mV in left atrial cells ($P<0.05$, *n*=8) (Fig. 1B). Adenosine significantly shortened the mean APD_{90} by 31±4 %

(P<0.05, n=14) and 30±7 % (P<0.05, n=8), in AV nodal and left atrial cells, respectively. This was associated with a corresponding decrease in the ERP in the left atrial cell (Fig. 1Aii), but not in the AV nodal cell (Fig. 1Ai). The mean ERP of left atrial cells was significantly shortened by adenosine, from 124±15 to 98±14 ms (P<0.05, n=8), but there was no significant effect of adenosine on the mean ERP of AV nodal cells (112±13 vs 102±12 ms, n=14). This differential effect of adenosine on the mean ERP of AV nodal and atrial cells, in the presence of hyperpolarisation in both cell types, is illustrated in Fig. 1B. In contrast to the effect on left atrial cells, adenosine significantly increased post-repolarisation refractoriness in AV nodal cells: the ERP/APD_{90} ratio increased from 1.65±0.09 to 2.22±0.12 (P<0.05, n=14). In both fast and slow V_{max} AV nodal cells, adenosine caused a similar significant hyperpolarisation and APD-shortening, but with a similar lack of an effect on the ERP. In both types of AV nodal cell, there was also a similar significant increase in post-repolarisation refractoriness: the ERP/APD_{90} ratio was increased by adenosine from 1.54±0.13 to 2.13±0.15 (P<0.05, n=8) in the fast V_{max} cells, and from 1.79±0.13 to 2.33±0.22 (P<0.05, n=6) in the slow V_{max} AV nodal cells, respectively.

3.3. Effect of hyperpolarisation on AV nodal and atrial cell refractoriness

Fig. 2A shows the effects of injecting hyperpolarising current into an AV nodal and a left atrial cell. This current was intended to mimic the effect on membrane potential of the adenosine-induced current, I_{KAdo}, and its magnitude was adjusted to hyperpolarise each cell by the mean value recorded in response to 10 μM adenosine, ie: by approximately 7 mV. The AV nodal cell illustrated may have been a transitional cell, since hyperpolarisation caused an increase in V_{max}, presumably by recruiting previously unavailable Na^+ channels. The mean current injected in AV nodal cells (n=7) and left atrial cells (n=8) was 14±5 and 22±4 pA, respectively. The mean magnitude of hyperpolarisation which resulted (Fig. 2B) was similar to that caused by adenosine in both groups of cells (Fig. 1B). Hyperpolarising current, like adenosine, shortened APD_{90} in both cell types, but the effect on APD was not as marked as that of adenosine: the APD_{90} shortened by 14±6 % (P<0.05, n=7) in AV nodal cells, and by 15±3 % (P<0.05, n=8) in left atrial cells. As with adenosine, there was associated shortening of mean ERP in left atrial cells. However, in contrast to the action of

adenosine, hyperpolarising current significantly shortened the ERP in AV nodal cells also. This is shown in Fig. 2B (compare with Fig. 1B). Mean ERP in AV nodal and left atrial cells was 146±12 (*n*=7) and 124±6 ms (*n*=8), respectively and hyperpolarising current significantly reduced this in both cell types, to 121±13 and 104±6 ms ($P<0.05$), respectively. Also, in contrast to actions of adenosine, hyperpolarisation did not modify post-repolarisation refractoriness in AV nodal cells: the ERP/APD_{90} ratio was 1.53±0.06 (*n*=7) in the absence of hyperpolarisation and 1.45±0.09 in its presence (*n*=7).

3.4. Effect of adenosine and hyperpolarisation on threshold current

The effects of adenosine (10 μM) and hyperpolarising current on cell excitability, assessed by the magnitude of stimulus current required to reach threshold, are shown in Fig. 3. In both the AV nodal and the left atrial cell, adenosine and hyperpolarising current caused an increase in this threshold current (Fig. 3A). The AV nodal cell illustrated may have been an A-N cell, owing to its to its relatively fast V_{max}. The mean threshold current in the absence of an intervention was 139±28 pA (*n*=10) in AV nodal cells and 219±86 pA (*n*=8) in left atrial cells. Fig. 3B shows that adenosine increased the mean threshold current in left atrial cells (*n*=8). A similar trend was seen in AV nodal cells (*n*=7). However, the effect of adenosine was not consistent in all cells: in 3 cells, the threshold current actually decreased. The resulting scatter of data meant that the effect on the mean threshold current did not reach significance. Fig. 3B also shows that hyperpolarising current caused a significant increase in the mean threshold current in AV nodal cells (*n*=10) and in left atrial cells (*n*=8).

3.5. Effects of adenosine on I_{CaL} in AV nodal cells

Fig. 4A shows recordings of I_{CaL} from a representative AV nodal cell. The voltage clamp protocol used is shown above the current traces, and is represented diagrammatically in Fig. 4B (inset). The 1 s long conditioning pulse ("c", of Fig. 4A) was used to activate, then completely inactivate I_{CaL}. As the interval between this pulse and a subsequent 300 ms long test pulse (eg: "t_1", of Fig. 4A) was progressively

increased, the amplitude of I_{CaL} evoked by the test pulse increased, as I_{CaL} recovered from inactivation. The magnitude of peak I_{CaL} was measured 3 s after the end of the conditioning pulse (eg: at "*t*=3 s" in Fig. 4A), at which time I_{CaL} had fully recovered in all cells studied, and was averaged in each cell, from 3 recordings. The mean current density of peak I_{CaL} was 30.3±3.8 pA/pF in a group of AV nodal cells (*n*=5). In the presence of adenosine (10 μM), this was not significantly different, at 27.9±3.7 pA/pF (*P*=0.101). Following washout of adenosine, the current density was 24.0±3.1 pA/pF. In each cell studied, no reduction by adenosine of peak I_{CaL} could be distinguished from the small degree of current rundown which was observed over the course of each 20-30 min experiment.

In contrast to the lack of effect of adenosine on the amplitude of peak I_{CaL}, the time course of recovery of I_{CaL} from inactivation was altered by adenosine. There was a reduction by adenosine in the amplitude of I_{CaL} at short interpulse intervals, in contrast to the effect with a 3 s interval (Fig. 4A). For each of the AV nodal cells studied, peak I_{CaL} amplitude was plotted graphically at each interpulse interval, as a function of the maximum peak amplitude recorded. Each resulting curve, representing the recovery of I_{CaL} from inactivation, displayed a biexponential time course. The data for each curve closely fitted a biexponential curve described by the equation given in Methods. The mean time course of recovery of I_{CaL} from inactivation in AV nodal cells is shown in Fig. 4B. The first (fast) phase of recovery of I_{CaL} from inactivation had a time constant (τ_1) of 102±10 ms (*n*=5), and 71±3 % of the recovery occurred in this phase. The second (slow) phase of recovery of I_{CaL} from inactivation had a time constant (τ_2) of 858±168 ms (*n*=5), and 31±3 % of the recovery occurred in this phase.

The effect of adenosine (10 μM) on the mean time course of recovery of I_{CaL} from inactivation in AV nodal cells (*n*=5), and its complete reversal following washout of adenosine is shown in Fig. 4B. In each AV nodal cell, adenosine (10 μM) had little or no effect on the time constant of either the fast or slow phase of recovery of I_{CaL} from inactivation, but reduced the proportion of recovery from inactivation within the fast phase, and increased the proportion of recovery within the slow phase. This is illustrated in Fig. 5B, which shows the lack of effect of adenosine on the mean time constant in each phase of recovery of I_{CaL} from

inactivation. In contrast, adenosine caused a significant shift in the mean proportion of recovery of I_{CaL} from inactivation from the fast, to the slow phase (Fig. 5A). At intervals corresponding to the AV nodal ERP, the magnitude of I_{CaL} was significantly reduced by adenosine (eg: by 17.8±3.6 %; $P<0.05$, at 100 ms, and by 14.1±3.5 %; $P<0.05$, at 120 ms; see Fig. 4*B* inset). Similar results were obtained from left atrial cells: as with the AV nodal cells, adenosine did not alter the time constant of either the fast or slow phases of recovery of I_{CaL} from inactivation (81±3 and 888±343 ms, respectively; $n=4$), but shifted the proportion of recovery of I_{CaL} from inactivation, from 81±3 to 50±5%, and from 21±2 to 53±5%, in the fast and slow phases, respectively ($n=4$, $P<0.05$).

To assess the effect of hyperpolarisation of the membrane on the recovery of I_{CaL} from inactivation, the holding potential was shifted from -40 mV to -47 mV in a separate group of AV nodal cells ($n=5$). The proportion of recovery of I_{CaL} from inactivation was unaffected by the change in holding potential in either phase of recovery (65±10 and 36±10 % at -40 mV, and 68±4 and 35±4 % at -47 mV, in the fast and slow phases, respectively). There was a decrease in the time constant of the fast phase, from 84±7 to 61±1 ms ($P<0.05$), but no significant shift in the time constant of the slow phase. The magnitude of I_{CaL} at intervals corresponding to the ERP was not significantly altered by these changes ($P>0.05$, $n=5$). A potential contamination by other inward currents (I_{Na} or T-type Ca^{2+} current) at the more negative holding potential was excluded, since 5 μM nifedipine ($n=5$ cells) abolished I_{CaL} in each cell, with no additional inward currents evident at either holding potential.

4. Discussion

We have demonstrated a differential effect of adenosine on refractoriness in AV nodal and atrial cells, which related to different consequences in the two cell types of actions of adenosine on I_{KAdo} and I_{CaL}. Adenosine, whilst causing marked and comparable shortening of APD in both cell types, shortened the ERP in left atrial cells, but not in the AV nodal cells. Thus, a novel finding of this study, is that post-repolarisation refractoriness, which is a property of AV nodal cells [14], was increased by adenosine, and may be related to a slowing by adenosine of the recovery of I_{CaL} from inactivation. The ERP-shortening effect of adenosine in the atrial cells is consistent with the shortening of the APD which we and others [7] have observed. Wang *et al*. [5], in a study of AV nodal cells, showed that adenosine, 1 μM caused a small prolongation of ERP. In our study an adenosine-induced prolongation of ERP was not observed, but post-repolarisation refractoriness was increased by adenosine. One difference between the two studies was that we used a higher concentration of adenosine, 10 μM, which caused a marked shortening of APD in the AV nodal cells which may have counteracted any prolongation of the ERP.

The AV nodal cells of the present study originated from the region of the AV node, and hence contained a heterogeneous mixture of AV nodal cell types, including mid-nodal, as well as transitional cells. The AV node is recognised to have a highly non-uniform structure, both in terms of cell morphology and electrophysiology [17] and a correlation between AV nodal single cell morphology, action potential shape and ion current characteristics has been reported [14]. Various morphological types of AV nodal cells have been described, including "ovoid-shaped" [14], as well as "spindle"- and "rod"- shaped cells [8,11,14,18,19]. Cell morphology and action potential shape may be similar in A-N and right atrial cells [14]. Thus, it was crucial to distinguish between AV nodal and atrial cells in the present study, and therefore the input resistance, which has consistently been demonstrated to be higher in AV nodal than atrial cells [5,8,14-16] (due to the lack of inward rectifier current, I_{K1}), was used for this purpose. The AV nodal cells we observed were "spindle" or "rod"-shaped, in agreement with previous data from our laboratory [8,11]. We did not observe "ovoid" cells, as described by Munk *et al.* [14]. The "fast V_{max}" AV nodal cells may be similar to the

A-N cells of that study, and the "slow V_{max}" cells may have been more mid-nodal in origin. The response to adenosine in both of these AV nodal cell subdivisions, was similar.

The present results provide insights into the ionic basis of the differential effect of adenosine on AV nodal and atrial cell refractoriness. It has been shown that adenosine-induced hyperpolarisation and APD shortening are associated with activation of a time-independent potassium conductance, I_{KAdo}, in atrial [7] and AV nodal [8] myocytes. It might be expected that the degree of adenosine-induced hyperpolarisation would differ in AV nodal and atrial cells, owing to the differing input resistance of these cell types. However, we observed a similar degree of hyperpolarisation in the atrial and AV nodal cells, which may indicate differences in the signal transduction mechanism of adenosine, including A_1 adenosine receptor density and reserve, or efficacy of G-protein coupling [20]. The contribution of I_{KAdo}-induced hyperpolarisation to the functional effects of adenosine was evaluated in the two cell types, by inducing an equal degree of hyperpolarisation to that produced by adenosine using current injection, thus isolating the hyperpolarising effects of I_{KAdo} activation from actions of adenosine on other membrane currents such as I_{Ca}. Hyperpolarising current produced shortening of the APD, but to a lesser degree compared to the effect of adenosine. This may reflect the fact that hyperpolarising current injection, whilst mimicking the effect of adenosine on resting membrane potential, would be unlikely to reproduce all of the consequences of activation of I_{KAdo}, which has a non-linear current voltage relationship. However, most importantly, there were corresponding reductions in ERP in both cell types, not just in left atrial cells, without changes of post-repolarisation refractoriness in AV nodal cells, in contrast to the increase with adenosine. Shortening of APD has been shown to be strongly correlated with activation of I_{KAdo} and weakly correlated with inhibition of I_{CaL} in guinea-pig atrial cells [10]. However, the differing responses of AV nodal refractoriness to hyperpolarising current and adenosine suggest an effect of adenosine on currents additional to hyperpolarising current, and may involve other currents, such as I_{Ca}.

Adenosine had no effect on peak I_{CaL} in AV nodal cells. Previous reports have indicated variable effects on peak I_{CaL}. For example, in a study on rabbit AV nodal cells [8], a small reduction of I_{CaL} was observed in

some cells, but with no significant effect on the mean I_{CaL}. Also in rabbit AV nodal cells, a depression of I_{CaL} was demonstrated when using adenosine at concentrations higher than that required to activate I_{KAdo} [5]. Reduction in I_{CaL} magnitude in atrial cells has been reported in guinea-pig [21] and human [22]. Such reduction in peak inward current would slow conduction through intact nodal tissue, by depression of V_{max} [6], and may contribute to the negative dromotropic action *in vivo*, but an effect on peak I_{CaL} did not underlie the actions of adenosine on the refractoriness of single myocytes. The known indirect action of adenosine on catecholamine-stimulated I_{CaL} [11] may also be expected to have a contributory effect on the AV node *in vivo*, especially under conditions of elevated levels of catecholamines. It is of interest to note that the amplitude of I_{CaL} was higher in AV nodal cells in this study, than that previously reported [5,8,14,19]. These studies used the ruptured patch technique, and from our own experience with AV nodal cells [8], I_{CaL} was smaller and exhibited rapid rundown compared to the present results with Nystatin-permeabilised patches.

In contrast to the lack of effect of adenosine on I_{CaL} amplitude, adenosine caused slowing of the recovery of I_{CaL} from inactivation. The recovery time course was biexponential, with characteristics similar to those reported previously [19,23]. We found that adenosine had no effect on the time constant of either phase of recovery in AV nodal cells, in agreement with reports on guinea-pig atrial myocytes [21] and a sinoatrial nodal multicellular preparation [24]. However, adenosine altered the proportion of recovery of I_{CaL} which occurred in each phase, causing a shift from a fast, to a slow recovery phase. Since such slowing of recovery occurred at intervals which correspond to the ERP in these cells, this may underlie the observed actions of adenosine on AV nodal refractoriness. Adenosine's hyperpolarising effect might offset this action on I_{CaL}, by reducing the time constant of the fast phase of recovery from inactivation. However, such an offset would only be partial, since shifting the holding potential from -40 to -47 mV had no significant effect on the proportion of recovery which occurred either in the fast and slow phases of recovery, nor on the magnitude of I_{CaL} recorded at intervals corresponding to the ERP.

The recovery of I_{CaL} from inactivation is a complex process, dependent on time, voltage and $[Ca^{2+}]_i$, with Ca^{2+} channels displaying several states of gating activity, including a long lived inactivated state which may last several seconds [25]. The two phases of recovery we observed may correspond to the distinct fast and

slow gating processes reported for Ca^{2+} channels of ventricular myocytes [26]. Single channel recordings of I_{CaL} from isoprenaline-stimulated ventricular myocytes have shown that adenosine, without altering unitary conductance, prolonged the time spent in an inactivated state. The transition rate from an activated to the inactivated state was enhanced and the recovery rate from the inactivated to the activated state was decreased [27]. Adenosine may have altered the gating of Ca^{2+} channels in the AV nodal cells in a similar manner. Stabilisation of the inactivated state of Ca^{2+} channels without change in unitary conductance also underlies use-dependent properties of Ca^{2+} channel blockers [28], some of which have similar effects on the AV node to adenosine [29]. In the present study, a direct effect of adenosine on channel gating, such as caused by Ca^{2+} antagonists, may have occurred but a mechanism requiring intracellular modulation of channel recovery kinetics, such as described by Kato *et al*. [27] seems more likely.

The effect of adenosine on I_{CaL} was similar in AV nodal and atrial cells, but may have had different consequences in the two cell types because of the differing role of I_{CaL} in the action potential of AV nodal cells. There is electrophysiological and histochemical evidence that I_{CaL} is the predominant inward current during depolarisation in these cells [6,30]. Therefore, slowing of recovery of I_{CaL} from inactivation by adenosine may affect refractoriness in AV nodal cells, in contrast to atrial cells, in which I_{Na} is the main inward current. Adenosine would not be expected to substantially alter ERP in atrial cells, due to the fast recovery of I_{Na} from inactivation [31]. Our findings support the suggestion, from studies of intact hearts, that an effect of adenosine on recovery of I_{CaL} from inactivation is likely to contribute to the negative dromotropic action of adenosine on the AV node [4]. One further factor to be considered is the unknown effect of adenosine on the T-type Ca^{2+} current (I_{CaT}). The magnitude of I_{CaT} in atrial cells was not altered by adenosine [21], but an effect on the time course of recovery of I_{CaT} has not been studied. Slowing of I_{CaT} may be the basis of "electrotonic inhibition" in the AV node [15] and such an action of adenosine might contribute to negative dromotropism in the AV node.

In addition to these effects on refractoriness, the effect of I_{KAdo} activation on excitability may contribute to the negative dromotropic effect of adenosine. Hyperpolarisation increased the threshold current in both cell types, indicating that adenosine-induced hyperpolarisation can decrease their excitability. In the intact node,

particularly with a high adenosine concentration, such an effect might account for the ability of adenosine to block impulse conduction. However, we observe that the effect of adenosine-induced hyperpolarisation on the excitability of single cells from the region of the AV node was variable. Due to the heterogeneous nature of the AV nodal cell population, some of the AV nodal cells would undoubtedly have contained Na^+ channels, of varying density, with absence of I_{Na} in cells from the compact node [30]. This is in contrast to the population of atrial cells studied, in which I_{Na} would always have been present. The increased excitability with adenosine in some cells may be related to this variation in the magnitude of I_{Na} between AV nodal cells from different regions [14]. Hyperpolarisation of a transitional cell, for example, whose diastolic potential is relatively depolarised compared to atrial cells, may result in the recruitment of previously unavailable Na^+ channels, increasing its excitability. In the intact node, this effect may be offset by the decreased excitability and increased refractoriness of adjacent nodal cells. It is acknowledged that electrotonic interaction among the different cell types within the AV node [32], as well as its complex three dimensional structure and pattern of depolarising wave input [33] require that caution be applied when extrapolating data obtained from single AV nodal cells, to the AV node *in situ*.

In conclusion, we have demonstrated that adenosine caused hyperpolarisation, APD-shortening and slowing of recovery of I_{CaL} from inactivation, in both AV nodal and atrial cells, but prolonged post-repolarisation refractoriness in AV nodal cells only. This differential effect of adenosine on refractoriness in the two cell types could not be explained by effects on I_{KAdo}, but may be due to slowed reactivation of I_{CaL}, which is the predominant inward current in AV nodal but not left atrial cells.

Acknowledgements

We gratefully acknowledge the technical assistance of Julie Russell in the isolation of cardiac myocytes.

This work was supported by the British Heart Foundation.

References

[1] Belardinelli L, Shryock JC, Song Y, Wang D, Srinivas M. Ionic basis of the electrophysiological actions of adenosine on cardiomyocytes. Faseb J 1995;9:359-365.

[2] Lai WT, Lee CS , Wu JC, Sheu SH, Wu SN. Effects of verapamil, propranolol, and procainamide on adenosine-induced negative dromotropism in human beings. Am Heart J 1996;132:768-775.

[3] Rankin AC, Brooks R, Ruskin JN, Mcgovern BA. Adenosine and the treatment of supraventricular tachycardia. Am J Med 1992;92:655-664.

[4] Nayebpour M, Billette J, Amellal F, Nattel S. Effects of adenosine on rate-dependent atrioventricular nodal function: potential roles in tachycardia termination and physiological regulation. Circulation 1993;88:2632-2645.

[5] Wang D, Shryock JC, Belardinelli L. Cellular basis for the negative dromotropic effect of adenosine on rabbit single atrioventricular nodal cells. Circ Res 1996;78:697-706.

[6] Clemo HF, Belardinelli L. Effect of adenosine on atrioventricular conduction. 1: site and characterization of adenosine action in the guinea pig atrioventricular node. Circ Res 1986;59:427-436.

[7] Belardinelli L, Isenberg G. Isolated atrial myocytes: adenosine and acetylcholine increase potassium conductance. Am J Physiol 1983;244:H734-H737.

[8] Martynyuk AE, Kane KA, Cobbe SM, Rankin AC. Adenosine increases potassium conductance in isolated rabbit atrioventricular nodal myocytes. Cardiovasc Res 1995;30:668-675.

[9] Kurachi Y, Nakajima T, Sugimoto T. On the mechanism of activation of muscarinic K^+ channels by adenosine in isolated atrial cells: involvement of GTP-binding proteins. Pflugers Arch 1986;407:264-274.

[10] Visentin S, Wu SN, Belardinelli L. Adenosine-induced changes in atrial action potential: contribution of Ca and K currents. Am J Physiol 1990;258:H1070-H1078.

[11] Martynyuk AE, Kane KA, Cobbe SM, Rankin AC. Nitric oxide mediates the anti-adrenergic effect of adenosine on calcium current in isolated rabbit atrioventricular nodal cells. Pflugers Arch 1996;431:452-457.

[12] Neher E. Correction for liquid junction potentials in patch clamp experiments. Methods Enzymol 1992;207:123-131.

[13] Korn SJ, Marty A, Connor JA, Horn R. Perforated patch recording. Methods Neurosci 1991;4:364-373.

[14] Munk AA, Adjemian RA, Zhao J, Ogbaghebriel A, Shrier A. Electrophysiological properties of morphologically distinct cells isolated from the rabbit atrioventricular node. J Physiol 1996;493:801-818.

[15] Liu Y, Zeng W , Delmar M, Jalife J. Ionic mechanisms of electrotonic inhibition and concealed conduction in rabbit atrioventricular nodal myocytes. Circulation 1993;88:1634-1646.

[16] Hoshino K, Anumonwo J, Delmar M, Jalife J. Wenckebach periodicity in single atrioventricular nodal cells from the rabbit heart. Circulation 1990;82:2201-2216.

[17] Meijler FL, Janse MJ. Morphology and electrophysiology of the mammalian atrioventricular node. Physiol Rev 1988;68:608-647.

[18] Hancox JC, Levi AJ, Lee CO, Heap P. A method for isolating rabbit atrioventricular node myocytes which retain normal morphology and function. Am J Physiol 1993;265:H755-H766.

[19] Hancox JC, Levi AJ. L-type calcium current in rod- and spindle-shaped myocytes isolated from rabbit atrioventricular node. Am J Physiol 1994;267:H1670-H1680.

[20] Shryock JC, Belardinelli L. Adenosine and adenosine receptors in the cardiovascular system: biochemistry, physiology, and pharmacology. Am J Cardiol 1997;79:2-10.

[21] Cerbai E, Klöckner U, Isenberg G. Ca-antagonistic effects of adenosine in guinea pig atrial cells. Am J Physiol 1988;255:H872-H878.

[22] Pelzmann B, Machler H, Schaffer P, Rigler B, Koidl B. Adenosine inhibits the L-type calcium current in human atrial myocytes. Naunyn-Schmiedeberg's Arch Pharmacol 1995;351:293-297.

[23] Li GR, Nattel S. Properties of human atrial I_{Ca} at physiological temperatures and relevance to action potential. Am J Physiol 1997;272:H227-H235.

[24] Satoh H. Electrophysiological actions of adenosine and aminophylline in spontaneously beating and voltage-clamped rabbit sino-atrial node preparations. Naunyn-Schmiedeberg's Arch Pharmacol 1993;347:197-204.

[25] Pelzer D, Pelzer S, McDonald TF. Properties and regulation of calcium channels in muscle cells. Rev Physiol Biochem Pharmacol 1990;114:107-207.

[26] Richard S, Tiaho F, Charnet P, Nargeot J, Nerbonne JM. Two pathways for Ca^{2+} channel gating differentially modulated by physiological stimuli. Am J Physiol 1990;258:H1872-H1881.

[27] Kato M, Yamaguchi H, Ochi R. Mechanism of adenosine-induced inhibition of calcium current in guinea pig ventricular cells. Circ Res 1990;67:1134-1141.

[28] McDonald TF, Pelzer S, Trautwein W, Pelzer DJ. Regulation and modulation of calcium channels in cardiac, skeletal, and smooth muscle cells. Physiol Rev 1994;74:365-507.

[29] Stark G, Sterz F, Stark U, Bachernegg M, Decrinis M, Tritthart HA. Frequency-dependent effects of adenosine and verapamil on atrioventricular conduction of isolated guinea pig hearts. J Cardiovasc Pharmacol 1993;21:955-959.

[30] Petrecca K, Amellal F, Laird DW, Cohen SA, Shrier A. Sodium channel distribution within the rabbit atrioventricular node as analysed by confocal microscopy. J Physiol 1997;501:263-274.

[31] Wu MH, Su MJ, Sun SM. Comparative direct electrophysiological effects of propofol on the conduction system and ionic channels of rabbit hearts. Br J Pharmacol 1997;121:617-624.

[32] Spitzer KW, Sato N, Tanaka H, Firek L, Zaniboni M, Giles WR. Electrotonic modulation of electrical activity in rabbit atrioventricular node myocytes. Am J Physiol 1997;273:H767-H776.

[33] Hocini M, Loh P, Ho SY, Sanchez-Quintana D, Thibault B, De Bakker JMT, Janse MJ. Anisotropic conduction in the triangle of Koch of mammalian hearts: electrophysiologic and anatomic correlations. J Am Coll Cardiol 1998;31:629-636.

Figure legends

Fig. 1. Electrophysiology of AV nodal and left atrial isolated myocytes, and effects of adenosine. (*A*) Action potential recordings from (*i*) an AV nodal and (*ii*) a left atrial isolated myocyte, in the presence (right) and absence (left) of adenosine (10 μM). Superimposed action potentials elicited by the last of a train of 8 conditioning current pulses, S_1, delivered at a rate of 300 beats/min are shown. These are followed by increasingly premature stimuli, S_2, including the longest S_1-S_2 intervals to fail to elicit action potentials (ERP). Dashed lines=0 V. (*B*) Histograms showing mean effects of 10 μM adenosine (black columns), compared to control (open columns) on the maximum diastolic potential (MDP) and the ERP, from 14 AV nodal and 8 left atrial cells. The adenosine ERP data has been normalised to the control (100 %). Error bars denote SEM. * = a significant difference from control (P<0.05).

Fig. 2. Effects of hyperpolarising current on ERP in AV nodal and atrial myocytes. *(A*) Superimposed action potential traces, recorded in response to the S_1-S_2 stimulation protocol, from (*i*) an AV nodal and (*ii*) a left atrial cell, with (right) or without (left) hyperpolarising current. Dashed lines=0 V. (*B*) Histograms showing mean effects of hyperpolarising current (black columns), compared to control (open columns) on the maximum diastolic potential (MDP) and the ERP, from 7 AV nodal and 8 left atrial cells. The ERP data has been normalised to the control (100 %). Error bars denote SEM. * = a significant difference from control (P<0.05).

Fig. 3. Effects of adenosine and hyperpolarising current on threshold current. (*A*) Superimposed membrane potential responses evoked by progressively increasing (in 50 pA steps; 2 subthreshold, 2 suprathreshold) current pulses of 5 ms duration in AV nodal and left atrial cells. Control recordings=C; recordings in the same cell, with adenosine 10 μM=Ado, and hyperpolarising current=Hyp. Numbers beneath the voltage traces indicate the threshold current (pA) recorded in that experiment. Dashed lines=0 V. (*B*) Histograms showing effects of adenosine and hyperpolarising current on the mean threshold current, from groups of 7-10 AV nodal cells and groups of 8 left atrial cells. Abbreviations are the same as in *A*. Control and

intervention data are indicated by open and filled columns, respectively. All threshold current data has been normalised to the control (100 %). Error bars denote SEM. * = a significant difference from control (P<0.05).

Fig. 4. Effect of adenosine on the time course of recovery of I_{CaL} from inactivation in AV nodal cells. (*A*) Superimposed voltage and current traces from an AV nodal cell showing effects of adenosine (10 μM) on I_{CaL} evoked during a voltage clamp experiment. Upper panel shows superimposed voltage traces from the end of conditioning pulses (c) of 1 s duration, followed, at varying intervals, from 20 ms to 3 s, by test pulses (eg: t_1) of 300 ms duration. Dashed line=0 V. Superimposed recordings of I_{CaL} are shown below, illustrating the reduction in peak I_{CaL} as the interval between the conditioning and test pulses is progressively diminished. Recordings of fully recovered I_{CaL} (ie, at t=3 s) are shown, following breaks (//) in the traces. Recordings are shown in the absence of adenosine (Control) and following superfusion with 10 μM adenosine for 90 s (Ado). (*B*) Effect of adenosine (10 μM) on the time course of recovery of I_{CaL} from inactivation in AV nodal cells. Values are means (n=5) of peak I_{CaL} recorded at interpulse interval t (see voltage clamp protocol inset), expressed as a percentage of the maximum peak I_{CaL} (recorded at t=3 s). Data for control (open circles), adenosine treatment (closed circles) and recovery after adenosine removal (closed squares) were fitted by curves with biexponential timecourses (see Methods for curve equation). An expansion of the time-scale for the first 150 ms is shown in inset. Error bars denote SEM.

Fig. 5. Effect of adenosine on the characteristics of recovery of I_{CaL} from inactivation. (*A*) Effect of adenosine (10 μM) on the proportion of recovery of I_{CaL} from inactivation which occurred in the fast and slow phases, respectively (n=5). $Ymax_1$ and $Ymax_2$ represent the I_{CaL} amplitude plateaux, derived from the biexponential equation detailed in Methods. (*B*) Lack of effect of adenosine (10 μM) on the time constants (τ_1 and τ_2) for the fast and slow phases of recovery of I_{CaL} from inactivation, respectively (n=5). Data (means, with error bars denoting SEM) are shown for control (open columns), adenosine treatment (black columns) and recovery after washout of adenosine (hatched columns). * = a significant difference between control and adenosine-treated groups (P<0.05).

Fig 1A

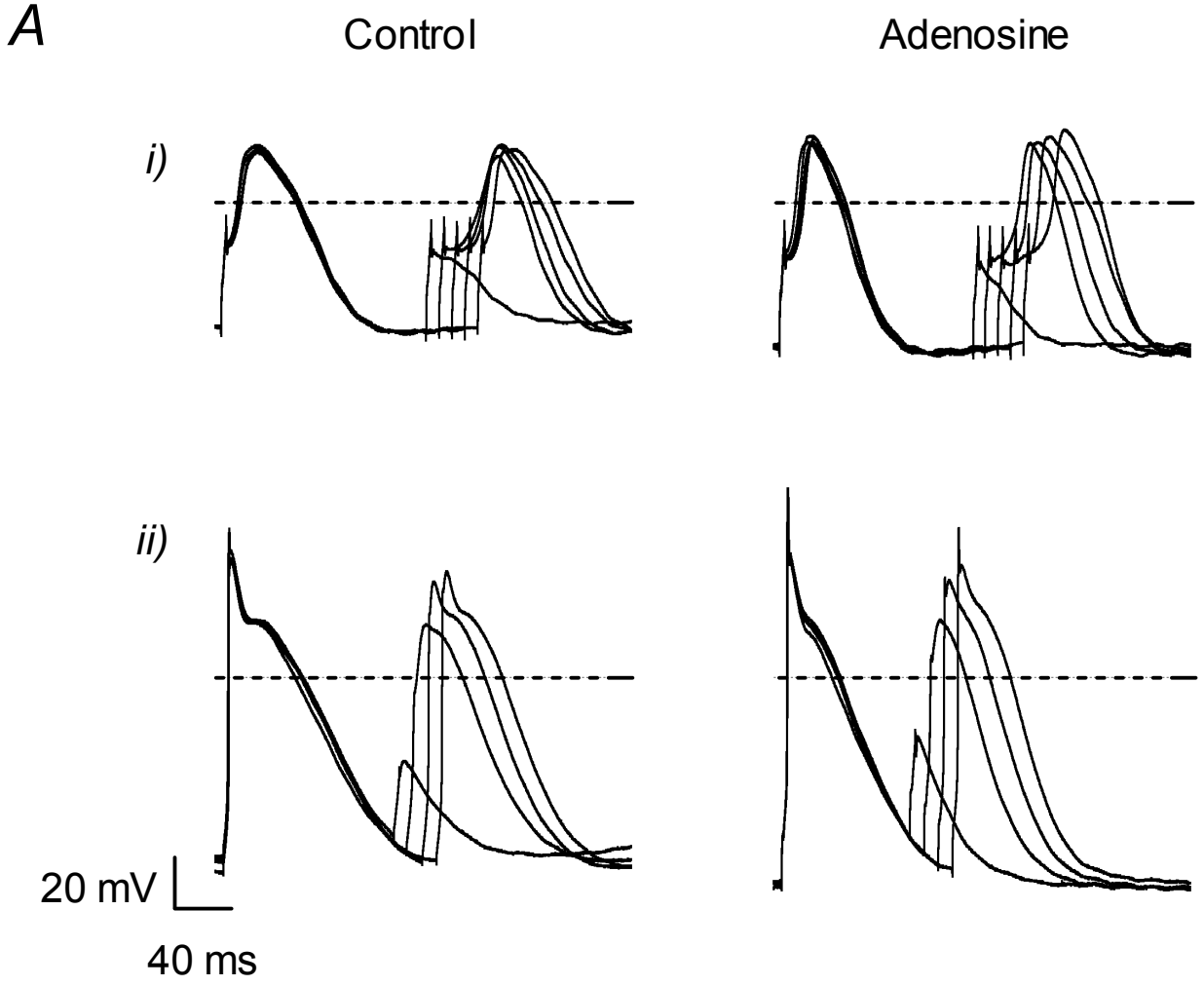

Fig 1B

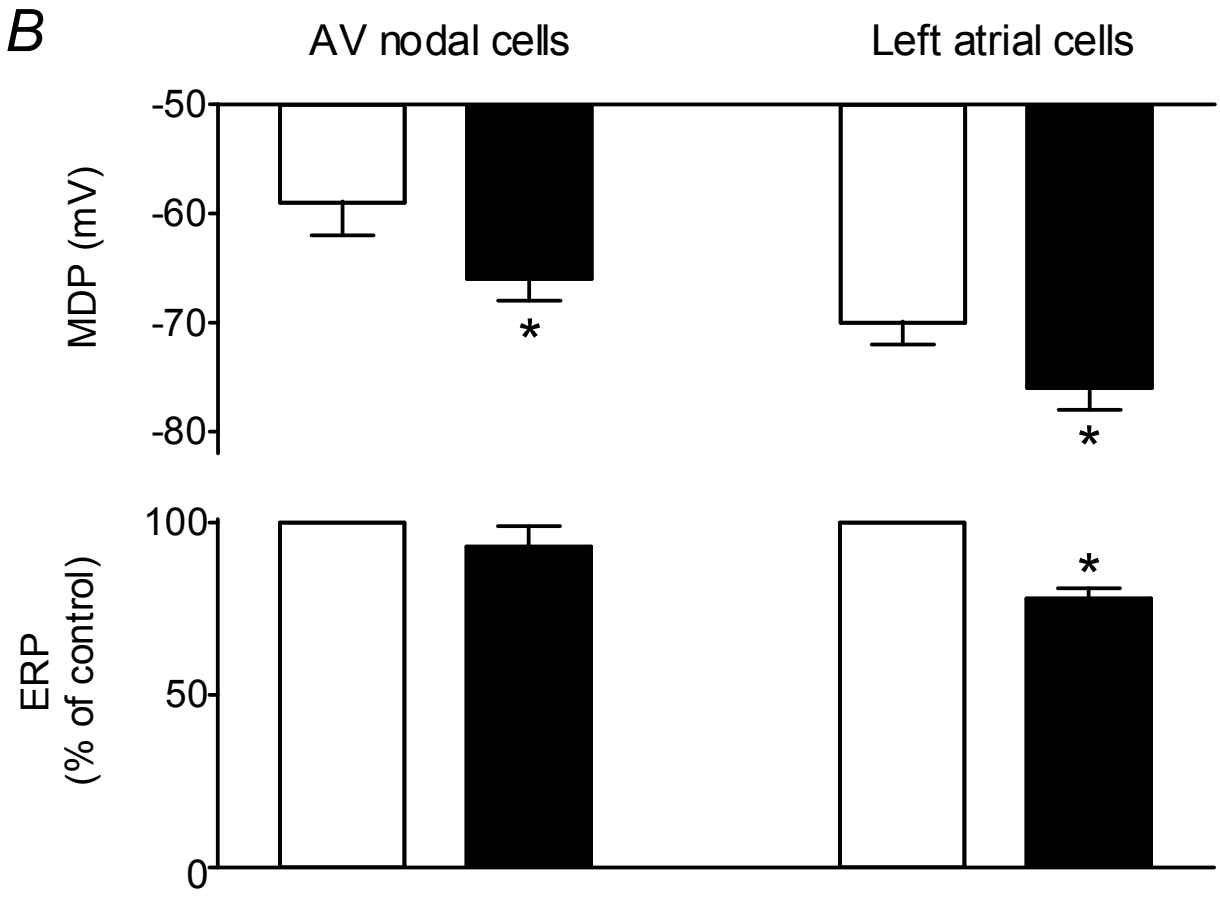
B
AV nodal cells
Left atrial cells
MDP (mV)
-50
-60
-70
-80
*
*
ERP
(% of control)
100
50
0
*

Fig 2A

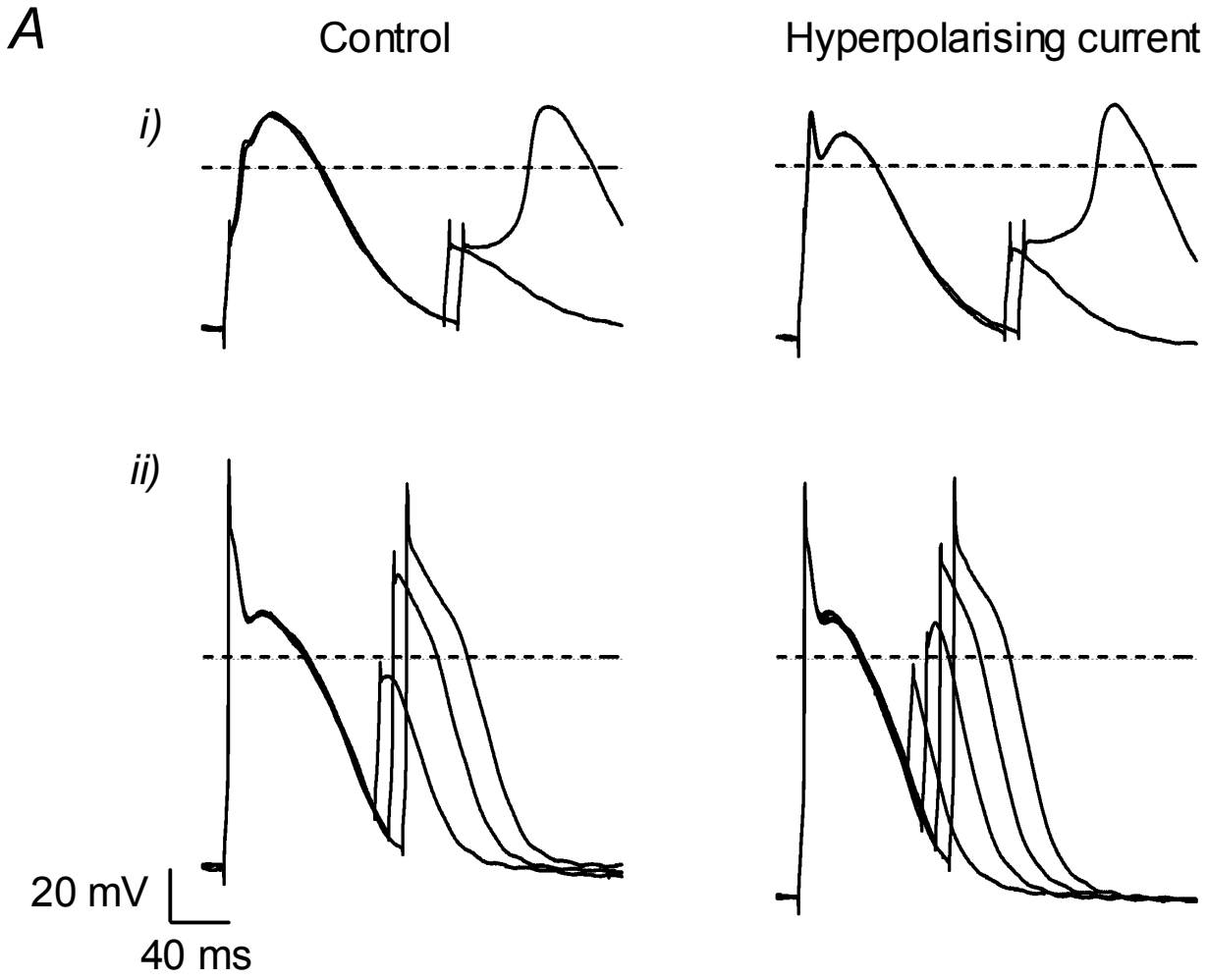

Fig 2B

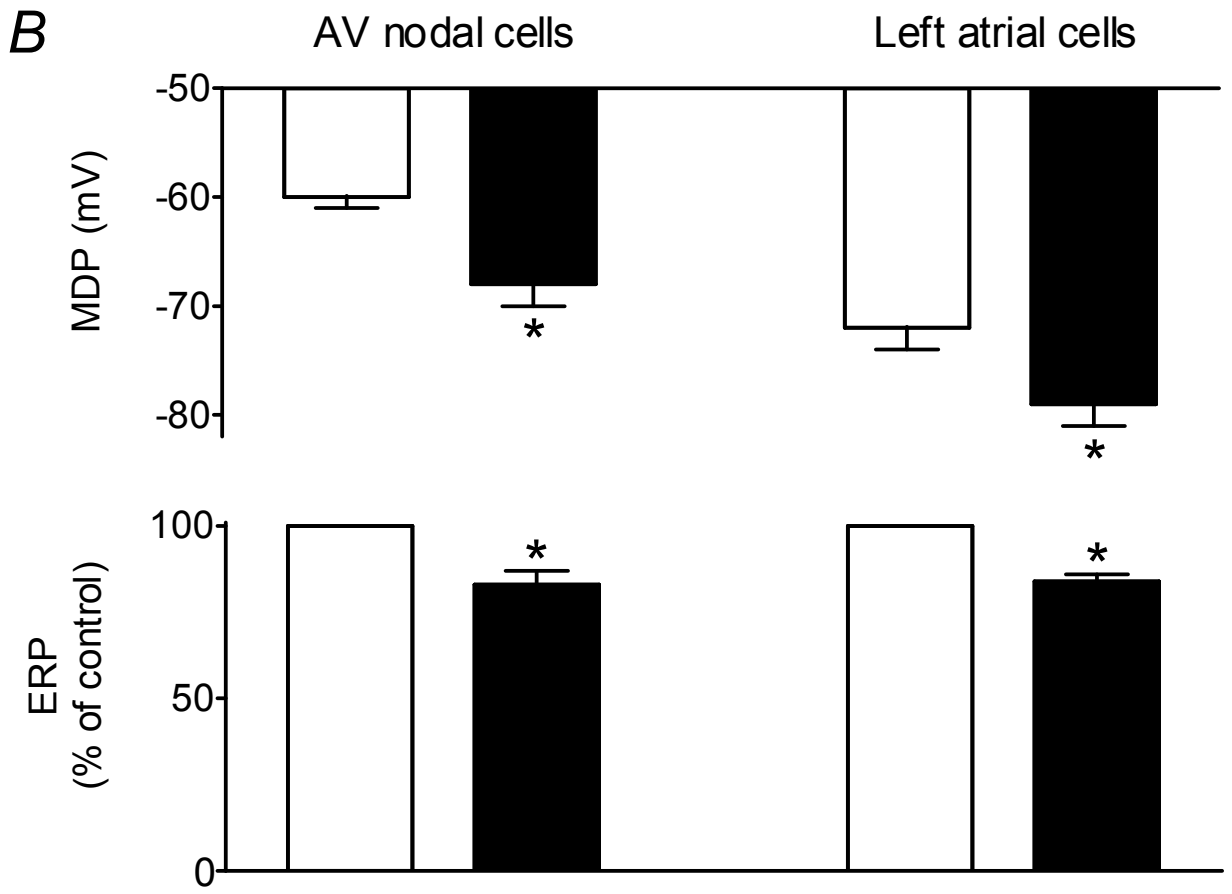
B
AV nodal cells
Left atrial cells
MDP (mV)
-50
-60
-70
-80
*
*
ERP
(% of control)
100
50
0
*
*

Fig 3A

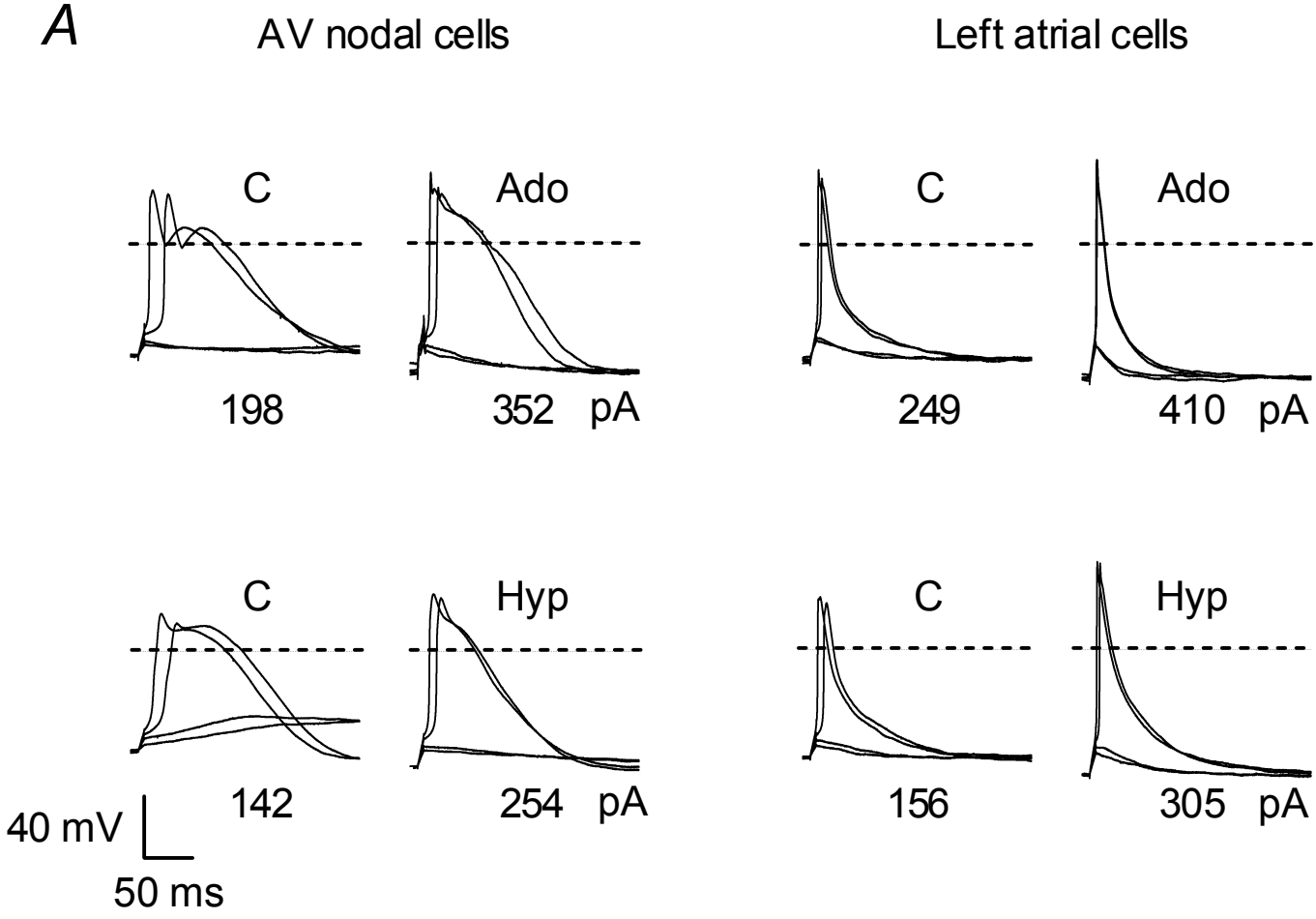
A
AV nodal cells
Left atrial cells
C
Ado
198
352 pA
C
Ado
249
410 pA
C
Hyp
142
254 pA
C
Hyp
156
305 pA
40 mV
50 ms

Fig 3B

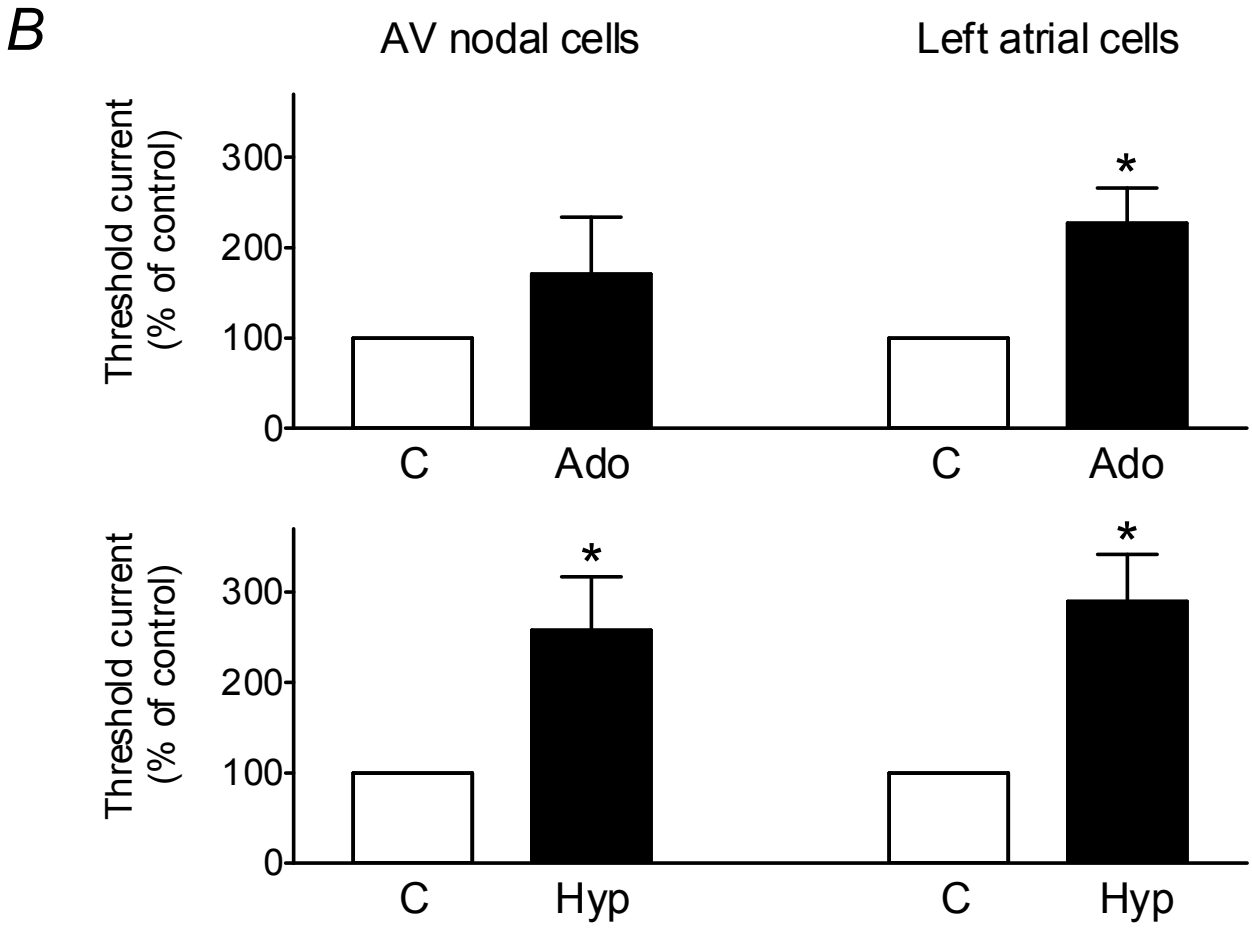
B
AV nodal cells
Left atrial cells
Threshold current (% of control)
300
200
100
0
*
C
Ado
C
Ado
Threshold current (% of control)
300
200
100
0
*
*
C
Hyp
C
Hyp

Fig 4A

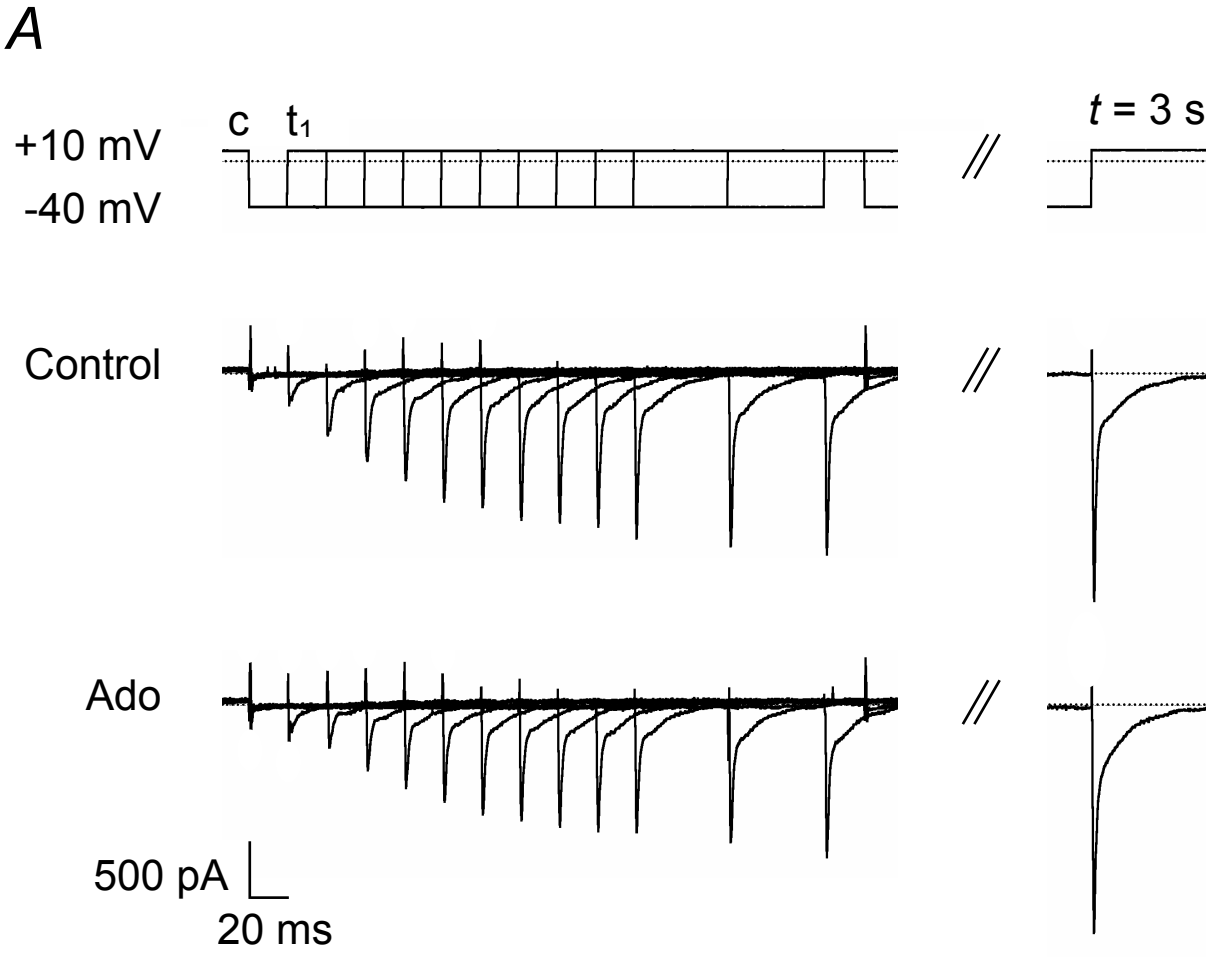

Fig 4B

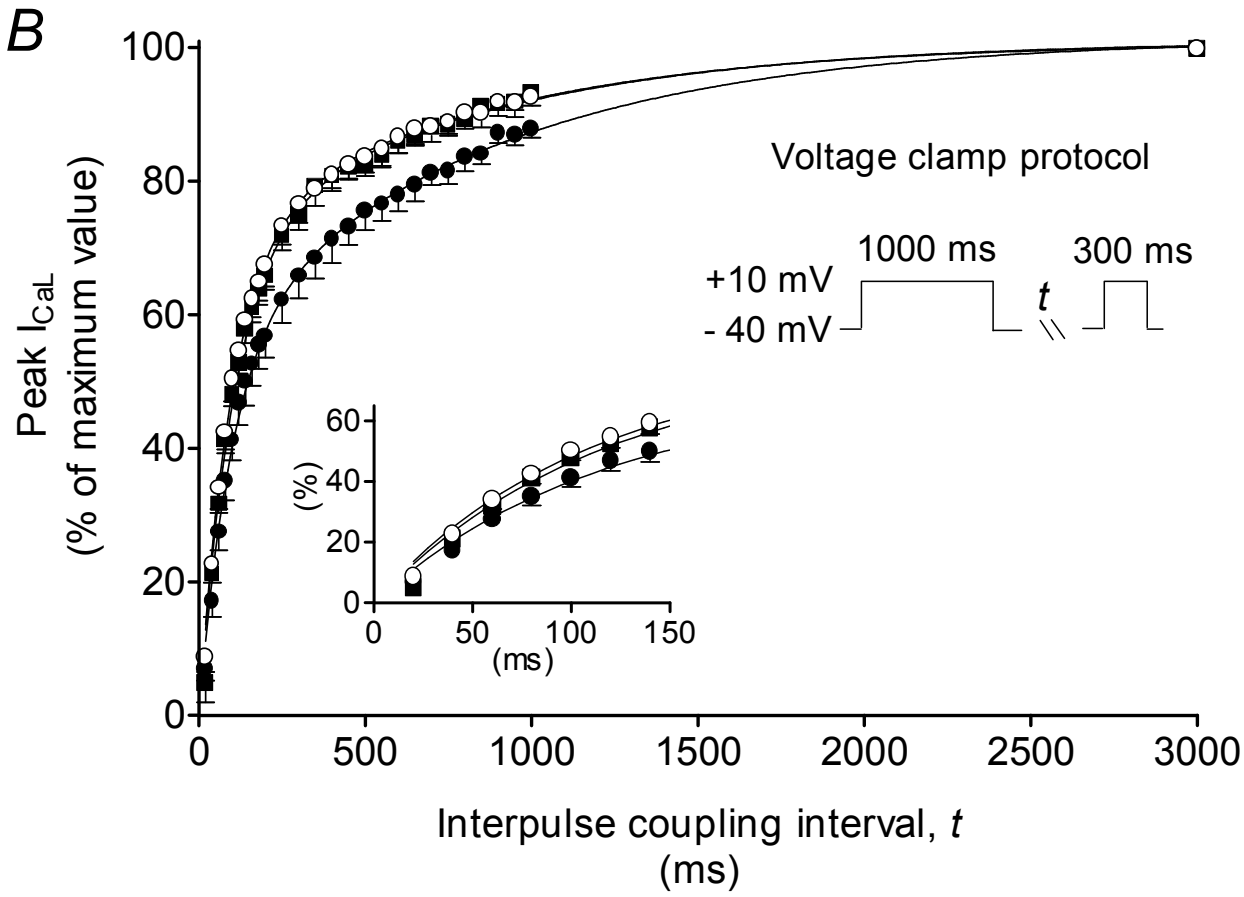
B
Peak I_{CaL}
(% of maximum value)
100
80
60
40
20
0
0
500
1000
1500
2000
2500
3000
Interpulse coupling interval, t
(ms)
Voltage clamp protocol
1000 ms
300 ms
+10 mV
- 40 mV
t
60
40
20
0
(%)
0
50
100
150
(ms)

Fig 5

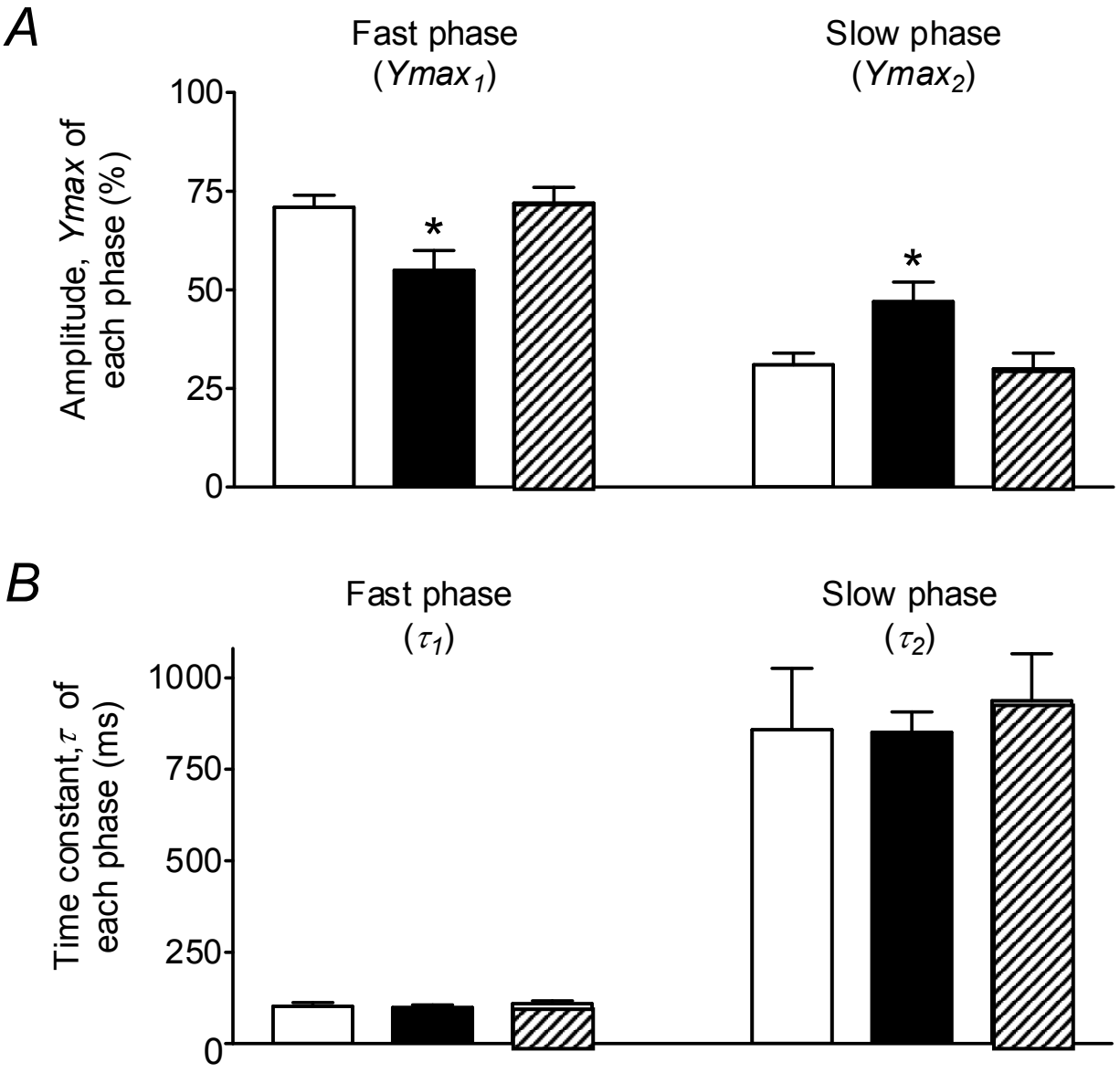
A
Fast phase
(Ymax1)
Slow phase
(Ymax2)
Amplitude, Ymax of each phase (%)
100
75
50
25
0
*
*
B
Fast phase
(τ1)
Slow phase
(τ2)
Time constant, τ of each phase (ms)
1000
750
500
250
0